

# Nonlinear refraction and absorption of Mg doped stoichiometric and congruent $\text{LiNbO}_3$

L. Pálfalvi

*Research Group for Nonlinear and Quantum Optics, Hungarian Academy of Sciences, H-7624 Pécs, Hungary*

J. Hebling<sup>a)</sup> and G. Almási

*Department of Experimental Physics, University of Pécs, H-7624 Pécs, Hungary*

Á. Péter, K. Polgár, K. Lengyel, and R. Szipöcs

*Research Institute for Solid State Physics and Optics, Budapest, P.O. Box 49, H-1525 Hungary*

(Received 27 June 2003; accepted 30 October 2003)

The light induced change of refraction is studied in pure and Mg doped  $\text{LiNbO}_3$  with congruent and stoichiometric compositions by the Z-scan method using all-lines visible argon ion laser, up to  $\text{MW}/\text{cm}^2$  intensity level. In Mg-doped congruent and stoichiometric crystals with Mg concentrations above threshold a positive change in the refractive index was found, in contrast to all other cases where beam fanning and negative change of the refractive index were observed. The beam distortion in the samples doped above threshold was related to thermal lensing, while below it to the photorefractive effects. It was also shown that for thermal lensing nonlinear absorption plays a dominant role. The Z-scan method was found to be an alternative technique to decide whether the Mg dopant level is above or below the photorefractive threshold. The damage resistance of the Mg doped samples above threshold was higher for the stoichiometric crystal than for the congruent one and increased with the amount of the built-in Mg concentration. © 2004 American Institute of Physics. [DOI: 10.1063/1.1635993]

## I. INTRODUCTION

Lithium niobate,  $\text{LiNbO}_3$  (LN) is one of the most frequently used nonlinear-optical materials, with various applications. Large crystals with congruent composition (Li/Nb ratio  $\sim 0.945$ ) have been readily available in excellent optical quality for several decades. Congruent lithium niobate crystals (cLN) possess photorefractive (PR) properties, which is a drawback in many fields of optics, since for device applications long-term stability of the beam is required. The unwanted PR damage of LN may be suppressed by certain dopants (like Mg, Zn, or In) added in concentrations exceeding a characteristic threshold level.<sup>1,2</sup>

Nowadays, by the preparation of bulk stoichiometric crystals with Li/Nb ratio of  $\sim 0.98-1$ , LN has a renaissance. Improvements of the material properties have opened the field for further investigations and applications. In stoichiometric LN (sLN) crystals the electro-optic and nonlinear-optic effects are reported to be more marked and the coercive field to be significantly lower than in cLN.<sup>3-5</sup> However, undoped sLN crystals exhibit weak optical damage resistance when irradiated with a high-power laser beam.<sup>6,7</sup>

So far, various methods have been used to characterize the optical damage resistance of LN crystals. Almost all monitor the light induced change in the refractive index. One of the most suitable experimental tools for this purpose is the Z-scan method.<sup>8</sup> Here a focused (Gaussian) beam illuminates the nonlinear material and the sample is scanned along the

propagation path around the focal plane. Information about the basic nonlinear characteristics of materials, namely the sign and magnitude of the nonlinear refraction ( $n_2$ ) and the coefficient of nonlinear absorption ( $\beta$ ), are deduced from the dependence of the far field on axis irradiance versus the position of the sample relative to the focal plane. Initially, this method was developed for “thin” nonlinear samples (for much shorter crystal length than the Rayleigh range of the focused laser beam). Later, it was completed for the case of thick samples.<sup>9</sup> The theoretical fitting formula of Ref. 9 contains  $n_2$  and  $\beta$  as independent fitting parameters. For thin samples  $\beta$  can be determined by the open-aperture Z-scan method as well.<sup>8</sup> For samples having thickness with the same order of magnitude as the Rayleigh range, the fitting formulas of Ref. 8 can be used only as an approximation, since the variations in the beam size are not taken into account.

In recent articles,<sup>10,11</sup> we examined the light induced change of refraction in LN by the Z-scan method and compared 5.0 mol % Mg doped cLN and sLN crystals. We found that using an all-lines visible argon ion laser, up to  $\text{MW}/\text{cm}^2$  intensity level, the stoichiometric crystals behave differently compared to congruent ones, namely the sLN sample shows positive (defocusing) and the cLN sample shows negative (focusing) change in the extraordinary refractive index. Such beam distortions can be the result of several effects. Besides photorefractive, the thermo-optical effect and at high beam intensity Kerr nonlinearity may lead to changes of the refractive index. While the light induced refractive index changes of Mg doped cLN crystal were related to the PR effect, in the

<sup>a)</sup> Author to whom correspondence should be addressed; electronic mail: hebling@fizika.ttk.pte.hu

case of Mg doped sLN crystals the thermal effect was found to be dominant.<sup>11</sup>

In this article we report some results on the light induced change of refraction also measured by the Z-scan method on a series of LN samples. The object of the following investigations is the characterization of the nature of the dominant effects resulting in different index changes for pure and doped stoichiometric and congruent LN crystals.

## II. EXPERIMENT

Our experimental setup was the standard single beam Z-scan setup described in Ref. 10. The Gaussian-beam source was an all-lines visible Ar-ion laser. In the experiments two lasers were used, labeled further as laser 1 and laser 2. Laser 1 was used in the whole power range: below 50 mW the dominant line was 488 nm, in the range of watts it worked with the 488 and 514 nm lines. Laser 2 was used only at 1.85 W power, working at 488 and 514 nm too. At 1.85 W power the relative weights of the 514 and 488 nm lines for laser 1 and laser 2 were 1.3 and 6, respectively. For the measurements three different lenses were used with a focal length of  $f=80, 91,$  and  $100$  mm, respectively. The beam waist, depending on the focal length of the lens, was between 15 and 18  $\mu\text{m}$ . The samples were scanned in the vicinity of the lens focus ( $z=0$ ) starting from a position ahead of focus ( $-z$ ) and moving toward a position behind the focus ( $+z$ ). The scanning range was about 25 mm in all cases. We recorded the laser power transmitted through a circular aperture located in the far field. The diameter of the aperture was much smaller than the beam size in the far field zone. To control the occurring temporal variation of the laser power, the total beam power was continually measured using a beam splitter placed in front of the lens. The Z-scan traces were obtained by plotting the normalized ratio of the power passing through the aperture and the total beam power. The coefficients of nonlinear refraction and absorption were determined from the fitting of the measured traces by the theoretical curve.<sup>9</sup> During the scanning charge coupled device (CCD) recordings of the beam cross sections were also done. The recordings were taken in the far field at distinct crystal positions: far from the focus, at the focus, at the minimum, and at the maximum of the Z scan. The analysis of the CCD recordings along two perpendicular directions was performed in detail. We used the Z-scan method for a quantitative characterization of the samples only in cases where a symmetric circular beam distortion was observed. For cases with elliptical distortion (fanning) on the transmitted beam spot, we also used the Z-scan arrangement for characterization of crystal properties, but instead of scanning the samples, we recorded the temporal evolution of the transmitted intensity in a fixed (postfocal) crystal position. For several samples the time evolution of the transmittance was in the  $\mu\text{s}$ –ms range and the observation was possible by oscilloscope. The nonlinear absorption of the samples was examined by open-aperture measurements as well.

The investigated samples are listed in Table I and labeled as Nos. 1–8. The congruent crystals (cLN) were prepared by the Czochralski technique. For the measurements nominally

TABLE I. Data for the congruent and stoichiometric  $\text{LiNbO}_3$  crystal samples.

Sample No.	Li/Nb ratio	Dopant concentration in the crystal (mol %)	Rise time of the optical damage measured with laser 1 $\tau$ (s)
1 sLN	0.999	—	4.3 (at 44 W/cm <sup>2</sup> )
2 cLN	0.945	$10^{-3}$ Fe	17.8 (at 44 W/cm <sup>2</sup> )
3 cLN	0.945	$10^{-2}$ Fe	5.6 (at 44 W/cm <sup>2</sup> )
4 cLN	0.945	—	12.6 (at 44 W/cm <sup>2</sup> )
5 cLN: Mg	0.945	5.0 Mg	38.6 (at 0.15 MW/cm <sup>2</sup> )
6 sLN: Mg	0.992	0.67 Mg	$\sim 10^{-3}$ (at 0.17 MW/cm <sup>2</sup> )
7 sLN: Mg	0.996	5.0 Mg	$\sim 10^{-3}$ (at 0.17 MW/cm <sup>2</sup> )
8 cLN: Mg	0.945	6.1 Mg	$\sim 10^{-3}$ (at 0.17 MW/cm <sup>2</sup> )

pure, Fe (0.001–0.01 mol %) and Mg (5.0–6.1 mol %) doped crystals were prepared. The stoichiometric (sLN) crystals were grown by the top seeded solution growth method from flux containing 12–13 mol %  $\text{K}_2\text{O}$ . Pure and Mg doped sLN crystals were prepared with dopant levels of 0.67 and 5.0 mol %, respectively.<sup>12</sup> The Li/Nb ratio in the undoped crystals was determined from the position of the UV absorption edge.<sup>13</sup> For doped crystals we assumed the ratio being identical with the value obtained for the undoped crystals grown under the same conditions. The built-in concentration of the dopants was determined by atomic absorption spectroscopy and is given in Table I. For all Mg doped crystals the level of compensation of Li vacancies in the lattice was checked by measuring the frequency of the  $\text{OH}^-$  vibration in the infrared (IR) spectra.

Experiments were performed on 2 mm thick Y-cut samples, except for crystal No. 6 from which both Y and Z cuts were tested. The samples were x-ray oriented with a precision better than  $0.5^\circ$ . The surfaces were polished with standard methods using 0.1  $\mu\text{m}$  diamond suspension. The examined samples were monodomain, crack, and inclusion free. In the measurements of the Y-cut samples the laser polarization was parallel to the optical axis ( $c$ ) of the crystal.

## III. RESULTS AND DISCUSSION

Optical properties of the LN crystals are improved by Mg doping. The characteristic threshold concentration to suppress the optical damage is reported to be above 4.6 mol % in cLN crystals.<sup>14</sup> This value is much lower in sLN since the threshold concentration is related to the way of the Mg incorporation. For concentrations below that critical threshold, Mg replaces  $\text{Nb}_{\text{Li}}$  antisite, while above it (where all antisites are already eliminated) Mg starts to replace  $\text{Li}_{\text{Li}}$ . This difference in the defect structure is manifested in abrupt changes of some physical properties.<sup>1,2</sup>

In the present study, the position of the IR absorption band of the  $\text{OH}^-$  stretch mode was used to decide whether the Mg concentration of doped samples was above or below the threshold.<sup>15</sup> For samples Nos. 1–5 (pure: Nos. 1, 4; nominally pure: Nos. 2, 3; and cLN doped with 5.0 mol % Mg: No. 5) the  $\text{OH}^-$  vibrational band at  $3482\text{ cm}^{-1}$  clearly establishes that these samples are below the threshold. For

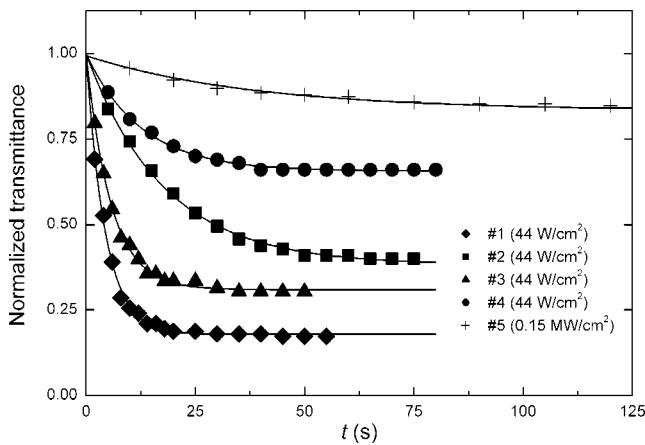


FIG. 1. The time dependence of the normalized transmittance at a fixed postfocal position for LN samples below threshold (Nos. 1–5) measured with laser 1.

all others (Mg doped sLN samples: Nos. 6–7 and No. 8: cLN doped with 6.1 mol % Mg) the  $\text{OH}^-$  peak is near  $3535\text{ cm}^{-1}$ , thus they are doped above threshold.

### A. Z-scan study of samples doped below threshold

In the course of the Z-scan measurements of pure and Fe doped cLN samples (Nos. 1–4), in postfocal positions the beam cross sections were strongly elongated along the optical axis of the crystal even for beam power lower than 1 mW ( $\sim 100\text{ W/cm}^2$  intensity). For 5.0 mol% Mg-doped cLN crystal (No. 5) such beam distortion becomes significant only at power levels of Watts ( $\text{MW/cm}^2$  intensity level). This fanning effect made impossible the use of the Z-scan technique in a quantitative way to determine the nonlinear refraction coefficient ( $n_2$ ) of these samples. In the standard Z-scan theory it is supposed that the local change of refraction is proportional to the local intensity of the Gaussian beam:  $\Delta n(r, z) = n_2 \cdot I(r, z)$ . This cylindrical symmetric variation of the refraction must result in a circular-symmetric beam shape variation in the far field. The observed elliptical beam distortion suggests the PR origin of the effect.<sup>16</sup> The  $\Delta n(r, z)$  change of the refractive index due to the photorefraction is not directly proportional to the local intensity. Thus the light induced changes of refraction in the PR LN samples (Nos. 1–5) cannot be studied by the single-beam Z-scan method. This is possible only under homogeneous illumination.<sup>16–18</sup> Therefore, for the characterization of these samples (Nos. 1–5) the temporal evolution of the transmittance was recorded in a fixed postfocal position of the samples. The time dependence of the normalized transmittances is shown in Fig. 1 as measured with laser 1. The power (intensity) was  $0.3\text{ mW}$  ( $44\text{ W/cm}^2$ ) in the case of samples Nos. 1–4 and  $1\text{ W}$  ( $0.15\text{ MW/cm}^2$ ) for No. 5. The time constants given in Table I were determined from the fitting of the curves to the function of  $T(t) = A_1 + (1 - A_1) \cdot \exp(-t/\tau)$ . Comparing the transmittance in the stationary state ( $A_1$ ) we can state that the pure sLN (No. 1) is much more sensitive than the pure cLN (No. 4). The rise time ( $\tau$ ) of the PR damage is shorter for No. 1 than for No. 4 as well. These results are in good agreement with Ref. 6, but are in contrast with Ref. 7. Bian

in Ref. 17 states, that the time constant is inversely proportional to the light intensity, and depends on the concentration of the donors and acceptors. It was found that among the Fe doped crystals (Nos. 2–3) sample No. 3 with higher built-in Fe concentration has lower  $A_1$  and  $\tau$ , and is more sensitive than the sample (No. 2) having lower Fe doping concentration. In nominally pure LN crystals Fe may be present in residual concentrations thus increasing the PR damage. The Mg doped congruent sample (No. 5) seems to be significantly less sensitive than the other PR samples (Nos. 1–4). For this sample the value of  $\tau$  and the stationary transmittance value is the largest even for beam intensities more than 3 orders of magnitude larger.

### B. Z-scan study of samples doped above threshold

The beam shape of Mg-doped samples (Nos. 5–8) does not show any changes for low light power. To observe any effect, application of  $\sim 1\text{ W}$  power level ( $\text{MW/cm}^2$  intensity level) was necessary. For both the Mg-doped sLN (Nos. 6–7) samples and the heavily Mg-doped cLN (No. 8) sample, the saturation times were on the  $\mu\text{s}$ – $\text{ms}$  scale and the observation of the evolution of the transmittances was possible only by an oscilloscope. In postfocal positions the temporal behavior of the transmittance is increasing, while in prefocal positions it is decreasing. Using  $2\text{ W}$  power the saturation time was slightly shorter than  $1\text{ ms}$ . Thus the time constant of Mg-doped sLN (No. 6) is 4 orders of magnitude shorter than that of the photorefractive samples (Nos. 1–5). Beside this significant difference, the transmittance in time evolves oppositely for samples above threshold Nos. 6–8 in the same (e.g., postfocal) position. This is in accordance with the previously reported observation on the congruent and stoichiometric cLN crystals doped with 5.0 mol % of Mg.<sup>10</sup> CCD recordings of the beam cross section of samples Nos. 6–8 also show that the beam distortion is circularly symmetric. Thus the analysis of the CCD recordings justifies the use of the Z-scan method for the quantitative characterization of these samples.

The Z-scan traces of Mg doped cLN samples (Nos. 5 and 8) are shown in Fig. 2 (measured with laser 1). A lens with a focal length of  $f = 80\text{ mm}$  was used in each case, and the laser power was  $400$  and  $1850\text{ mW}$  for Nos. 5 and 8, respectively. Although samples Nos. 5 and 8 differ only slightly in the level of the incorporated amount of Mg (Table I), the peak–valley configuration (sign) of the traces are different. The Z-scan trace of sample No. 8 is similar to that of the Mg doped sLN samples Nos. 6–7 (see Fig. 3 for measurements on No. 6 with laser 1 and Ref. 10 for No. 7). The sign of the Z-scan trace of sample No. 5 refers to photorefraction.<sup>17,18</sup> From this fact we can conclude that although for the cLN crystal with 5.0 mol % Mg dopant level photorefraction was significantly reduced (at  $400\text{ mW}$  power the beam distortion was much lower than for the pure LN) but still present.

The trace of the cLN sample No. 8 having a higher (6.1 mol %) Mg dopant level (Fig. 3) and those of the Mg-doped sLN samples (Nos. 6–7) show that in these samples PR may be absent or compensated for by some other effect.

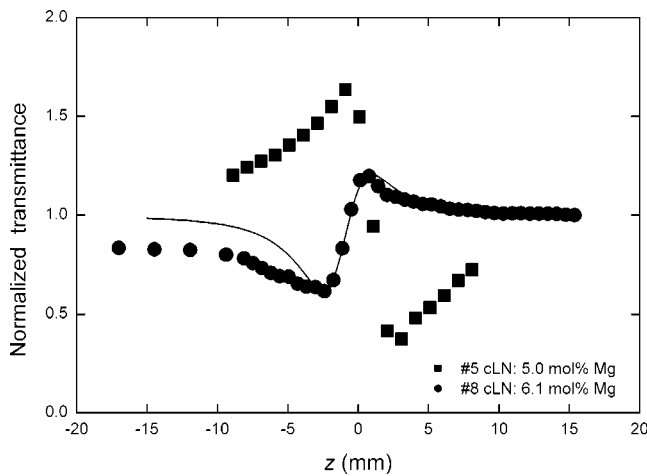


FIG. 2. Z-scan trace of congruent LN crystals doped with Mg in concentration below (squares) and above (circles) threshold, samples Nos. 5 and 8 measured with laser 1. The intensities were 60 and 270 kW/cm<sup>2</sup> for sample Nos. 5 and 8, respectively.

For both of the investigated Mg doped cLN samples (Nos. 5 and 8) the incorporated amount of Mg (given in Table I) is above the 4.6 mol % threshold concentration, reported to suppress the PR damage of cLN.<sup>14</sup> For sample No. 5 (cLN doped with 5.0 mol % Mg) the shift in the OH<sup>-</sup> frequency clearly established that this sample is still below the critical threshold, while No. 8 (cLN doped with 6.1 mol % Mg) is above the threshold. That difference between samples Nos. 5 and 8 explains the different sign of the Z-scan traces (taken at the pre- and postfocal positions) and also the 4 orders of magnitude difference in the saturation time constants. Thus there is a correlation between the position of the IR absorption band of the different samples and the sign of the corresponding Z-scan traces. For the Mg doped stoichiometric LN crystals (both Nos. 6 and 7), the IR absorption spectra in accordance with the Z-scan measurements showed that they are above the threshold. Accordingly the Z-scan measurement can be used as well to characterize

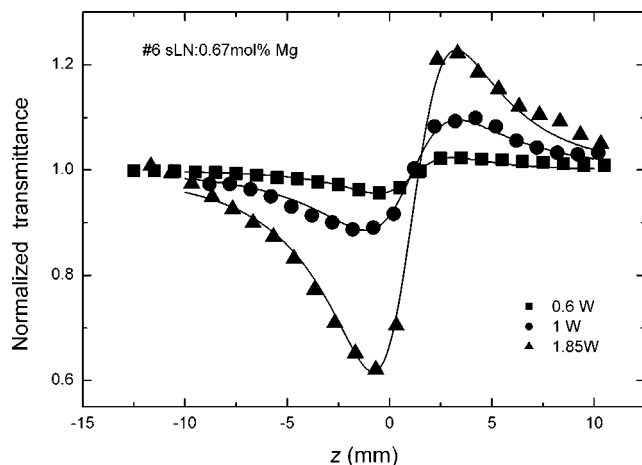


FIG. 3. Z-scan traces of stoichiometric LN crystal doped with 0.67 mol % Mg (sample No. 6) measured with laser 1 at different incident light powers ( $P=0.6, 1, 1.85$  W,  $f=100$  mm).

crystals having different Mg doping level, since the peak–valley configuration distinguishes samples above and below the PR threshold.

In order to compare quantitatively the nonlinear refraction of the Mg doped samples above threshold, we performed Z-scan measurements under the same circumstances using laser 1 with 1850 mW beam power and a focusing lens with focal length of 80 mm. The cLN crystal doped by 6.1 mol % Mg (No. 8) was found to be the most sensitive with  $n_2=1.4 \times 10^{-10}$  cm<sup>2</sup>/W and  $\beta=2.8 \times 10^3$  cm/GW values. For the 0.67 mol % Mg doped sLN sample (No. 6) we obtained  $n_2=1.3 \times 10^{-10}$  cm<sup>2</sup>/W and  $\beta=2.4 \times 10^{-3}$  cm/GW and for the 5.0 mol % doped sLN (No. 7) sample  $n_2=9.7 \times 10^{-11}$  cm<sup>2</sup>/W and  $\beta=1.7 \times 10^3$  cm/GW. Thus for the investigated Mg doped stoichiometric crystals both the nonlinear refractive index and the nonlinear absorption coefficient of the samples were smaller than for of the overthreshold congruent one and decreased with the amount of the built-in Mg concentration.

### C. The thermal effect and nonlinear absorption

The opposite signs of the extraordinary index changes of the Mg-doped samples below and above threshold suggests different origins of the effects. In the present experiments we can exclude the Kerr origin of the observed light induced refractive index change. The cw laser cannot induce measurable Kerr-type nonlinear refractive index changes<sup>11</sup> because of the modest peak power.

The peak–valley configuration of the Z-scan curves of the samples doped above threshold (Nos. 6–8) means positive value of  $n_2$ . The positive value of the temperature coefficient of the refractive index ( $dn/dT$ ) suggests a thermal origin of the change of refraction. Light absorption of a Gaussian beam causes a temperature distribution in the medium, which can be approximated (close to the optical axis), by a parabolic temperature profile. This causes a parabolic change in the refraction [see Eq. (4.2) of Ref. 19]

$$n = n_0 + \Delta n = n_0 + n_2 I = n_0 - 0.06 \alpha I_0 (dn/dT) r^2 / \pi \kappa. \tag{1}$$

Supposing the intensity profile to be also parabolic, that is  $n_2 I \approx n_2 I_0 \cdot (1 - 2r^2/w^2)$  one obtains

$$n_2 = 0.03 \alpha (dn/dT) w^2 / \kappa, \tag{2}$$

where  $\alpha$  is the linear absorption coefficient,  $\kappa$  is the heat conductivity, and  $w$  is the beam radius. According to Eq. (2) beside the material parameters  $n_2$  depends on the actual beam size too and during scanning the value of  $n_2$  changes. Thus constant  $n_2$  cannot be defined for a medium in which the nonlinearity originates from thermal effects,<sup>19</sup> more precisely, if only linear absorption is responsible for the effect. Such position-dependent  $n_2$  cannot be taken into account in the analytical fitting formula of Ref. 9. Furthermore our experimental results cannot be explained by linear absorption alone, as we have shown in previous work,<sup>11</sup> since using Eq. (2) we would obtain for  $n_2$  a value nearly ten times smaller than measured.

Recently, by open aperture measurement,<sup>8</sup> we have shown that the effect of nonlinear absorption is not negli-



TABLE II. Extraordinary nonlinear refractive index for sLN:0.67 Mg sample (No. 6) measured with laser 1 and lens with focal length of 100 mm.

$P$ (W)	Weight of the dominant lines 514 nm/488 nm	Measured $n_2$ ( $10^{-11}$ cm <sup>2</sup> /W)	Calculated $n_2$ ( $10^{-11}$ cm <sup>2</sup> /W)
0.6	1.05	6	5.1
1	1.3	10.9	8.4
1.85	1.3	17.3	15.5

gible for Mg-doped LN samples,<sup>10,11</sup> where 5–10% of the beam power was absorbed in the vicinity of the focus. Thus in the absorbance we may neglect the linear term beside the nonlinear one at high intensities. According to this, in Eq. (2)  $\alpha$  has to be replaced by  $I\beta = 2P\beta/w^2\pi$ , resulting in

$$n_2 = 0.06P\beta(dn/dT)/\pi\kappa. \quad (3)$$

Equation (3) in contrast with Eq. (2) gives a position independent  $n_2$ , which makes the theoretical fitting<sup>9</sup> possible. By fitting the trace of sample No. 8 shown on Fig. 2,  $n_2 = 1.4 \times 10^{-10}$  cm<sup>2</sup>/W, and  $\beta = 2.8 \times 10^3$  cm/GW was determined. Substituting this  $\beta$  value, the values of  $dn/dT$ , the  $\kappa$  material parameters, and the 1.85 W beam power applied in Eq. (3) we obtained  $n_2 = 1.6 \times 10^{-10}$  cm<sup>2</sup>/W. This is in good agreement with the value, which was determined from the fitting of the Z-scan trace. Equation (3) shows that  $n_2$  has to depend on the beam power. Therefore we performed Z-scan measurements on sample No. 6 using an achromatic lens with 100 mm focal length at three different laser powers (0.6, 1, and 1.85 W). The Z-scan curves are shown in Fig. 3 and the obtained  $n_2$  values are given in Table II. These results show the quasilinear dependence of  $n_2$  on beam power as predicted by Eq. (3). The averaged value of nonlinear absorption coefficients obtained as a second fitting parameter of the traces of Fig. 3 is  $2.6 \times 10^3$  cm/GW. Substituting this  $\beta$  value and the applied powers into Eq. (3) we obtain for  $n_2$  (calculated) very similar values to the directly fitted (measured) ones as shown in Table II.

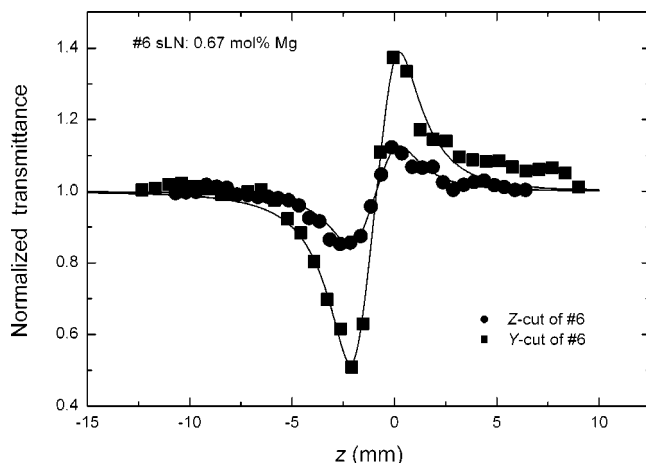


FIG. 4. Z-scan traces of stoichiometric LN crystal doped with 0.67 mol % Mg (sample No. 6) measured on samples cut perpendicular (Z-cut, circles) and parallel (Y-cut, squares) to the optical axis. Measured with laser 2,  $P = 1.85$  W,  $f = 91$  mm.

TABLE III. Nonlinear refraction characteristics for sLN: 0.67 Mg sample (No. 6) measured with laser 2 at 1.85 W and lens with focal length of 91 mm. Weight of the dominant lines 514 nm/488 nm  $\sim$ 6.

Sample orientation	$n_2$ ( $10^{-11}$ cm <sup>2</sup> /W)	$\beta$ ( $10^3$ cm/GW)	Maximal absorption
Y	13.4	1.7	39.7%
Z	4.3	0.55	11.9%
Ratio of the values (Y/Z)	3.11	3.09	3.3

According to Eq. (3) for constant applied beam power  $n_2$  is proportional to  $\beta$  as well. In order to verify this relation we performed Z-scan measurements on two different samples. Since the  $\beta$  values of samples Nos. 6, 7, and 8 were very similar we used the Y and the Z cut of sample No. 6. For this examination a lens with a focal length of 91 mm, and a different type of Ar-ion laser (laser 2) with beam power of 1.85 W was used. The results are depicted in Fig. 4. It is evident from the traces that for the Y-cut sample, the amplitude of the curve is about three times larger than for the Z cut. The ratio of the  $n_2$  values obtained from the fitting of the curves of Fig. 4 is found to be almost the same as the ratio of the obtained  $\beta$  values (see Table III). As indicated also by this result, it is mainly the nonlinear absorption, which is responsible for the formation of the thermal lens. While on sample No. 6 the measurements of the coefficient of nonlinear absorption gave  $2.6 \times 10^3$  cm/GW using laser 1, with laser 2 at the same power  $\beta = 1.7 \times 10^3$  cm/GW was obtained (Table III). This difference between the measured values can be explained by the diversity of the dominant lines of the lasers and the wavelength dependence of  $\beta$ .

To obtain independently the nonlinear absorption coefficient values of the Z and Y cuts of sample No. 6 we performed open-aperture measurements as well. The results are presented in Fig. 5. As shown, the maximally absorbed power is about three times larger for the Y-cut than for the Z-cut sample. In Fig. 5, the trace of the Y-cut sample shows the typical effect of the finite size of the aperture (similarly

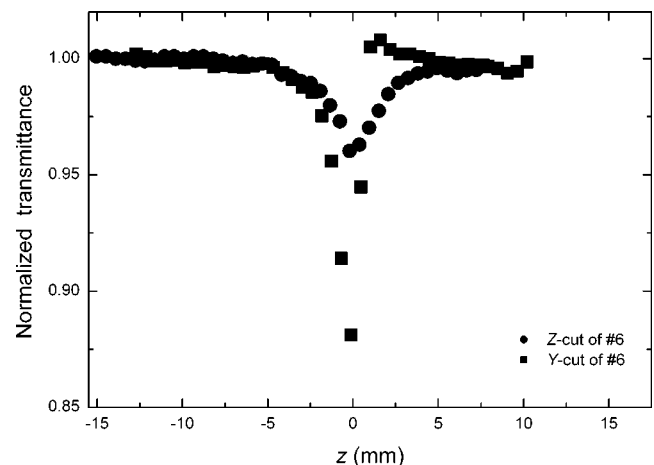


FIG. 5. Open aperture Z-scan trace of stoichiometric LN crystal doped with 0.67 mol % Mg (sample No. 6) measured on samples cut perpendicular (Z-cut, circles) and parallel (Y-cut, squares) to the optical axis. Measured with laser 2,  $P = 1.85$  W,  $f = 91$  mm.

to that of Fig. 9 of Ref. 8). For the Z-cut sample this effect disappears, although the measurement setup was totally the same. The maximally absorbed powers are indicated in Table III. Their ratio is in very good agreement with the ones obtained from the closed-aperture Z-scan fitting. These measurements further confirm that the nonlinear absorption plays a dominant role in thermal lensing. Furthermore, they also demonstrate the anisotropy of the nonlinear absorption; e.g., it depends on the relative orientation of the pump light and the crystal optical (*c*) axis.

The measured ms rise time of transmittance for sample No. 6 is also consistent with the estimated time of the warming up of Mg doped sLN. For that estimate we first determined the spatial temperature distribution in the crystal. Using Eq. (A8) of Ref. 20 and taking into account the nonlinear absorption, the heat conduction equation is

$$\frac{\beta I_0^2 w^2 2\pi}{8} \left( 1 - \exp\left(-\frac{4r^2}{w^2}\right) \right) \Delta z = -\kappa \frac{dT}{dr} 2r\pi \Delta z, \quad (4)$$

where  $I_0$  is the peak intensity and  $w$  is the beam size at a given slice ( $\Delta z$ ) of the material. Since the measurements were performed in postfocal and in prefocal points the beam size was supposed to be  $w = \sqrt{2}w_0$ . The steady state temperature distribution was determined by the

$$T(r) = T_0 + \frac{I_0^2 \beta w^2}{8\kappa} \int_0^r \frac{1}{x} \left( \exp\left(-\frac{4x^2}{w^2}\right) - 1 \right) dx \quad (5)$$

integral. This model has the weakness, that for points far from the optical axis, the temperature does not converge to a finite value. Thus we interpret the temperature increase of the middle part of the medium as the  $\Delta T$  temperature difference between the on axis point and a point far from the axis (e.g.,  $a = 10w$ ). In order to determine the time constant of the warming up process we determined the time, which was required to increase the temperature of a volume of the illuminated material. Since the small aperture measurement carries information about the region of the medium close to the optical axis, the radius of the warmed cylinder was supposed to be  $w/10$ . Inside this region the warming up ( $\Delta T$ ) of the material is nearly constant. The estimated time is

$$\tau = \frac{c\rho\Delta T}{I_0^2\beta} = \frac{c\rho w^2}{8\kappa} \int_0^a \frac{1}{r} \left( 1 - \exp\left(-\frac{4r^2}{w^2}\right) \right) dr, \quad (6)$$

where  $c$  is the specific heat and  $\rho$  is the mass density. Substituting  $w_0 = 18 \mu\text{m}$  and the values of  $c = 684 \text{ J/kg } ^\circ\text{C}$  and  $\rho = 4600 \text{ kg/m}^3$  for congruent LN from Refs. 21–22 into the above expression we obtain  $\tau = 0.2$  ms. Note that  $\tau$  is independent of  $\beta$  and  $I_0$ , since  $\Delta T \propto I_0^2 \beta$ . During the warming up process we neglected the heat conduction, although it was also present. The effect of the heat conduction during the warming up period results in a larger  $\tau$  than estimated. Our measured  $\tau$  is in good agreement with the theoretically predicted value. We consider it as another proof of the thermal origin of the effect.

In order to check that there is no residual photorefraction in this sample (No. 6) we performed a quick scanning and a slow one, waiting 1 min in every  $z$  position. The two traces totally overlapped each other, which means that all distortion passed off on the ms scale. This result demonstrates the absence of photorefraction, since the typical time constant of the transient is below 1 ms for the thermal effect and it is between 1 s and 1 min for photorefraction.

## IV. CONCLUSIONS

The light induced beam distortion for intensities up to  $\text{MW/cm}^2$  level was studied on a series of LN samples using a combination of single-beam Z-scan measurements with CCD recordings of the transmitted beam cross section and the observation of the temporal evolution of the transmittance in a fixed sample position. We found that in pure and nominally pure (containing Fe as impurity) cLN, sLN, and Mg-doped cLN with the Mg concentration below the threshold the PR effect is dominant and the Z-scan technique cannot be used in a quantitative way to determine the nonlinear refraction coefficient.

The Z-scan curves of crystals doped above the threshold show positive refractive index changes, opposite to those found below the threshold. Thus, the Z-scan measurement can also be used to distinguish crystals with Mg doping level above and below the photorefraction threshold.

For Mg doped sLN and cLN crystals, doped above the threshold, the PR effect was practically absent. The threshold concentration of the incorporated Mg was between 5.0 and 6.1 mol % for cLN, and lower than 0.67 mol % for sLN crystals. The laser resistance of the Mg doped samples above the threshold was higher for the stoichiometric crystal than for the congruent one and increased with the amount of the built-in Mg concentration.

The positive sign of the Z-scan traces and the order of magnitude of the measured nonlinear refractive index values ( $n_2$ ) indicate that the damage is of thermal origin. From the intensity dependence of  $n_2$  and from the results of combined Z-scan and open aperture measurements, we can conclude that the light absorption at the  $\text{MW/cm}^2$  level is mainly nonlinear.

## ACKNOWLEDGMENTS

Support from the Hungarian Scientific Research Fund Grant Nos. T038372, T034176, and T034262, the Hungarian Ministry of Education Grant No. DDKKK/2000 and Széchenyi NSRF No. 3/064 are kindly acknowledged.

<sup>1</sup>K. Polgár, L. Kovács, I. Földvári, and I. Cravero, *Solid State Commun.* **59**, 375 (1986).

<sup>2</sup>T. Volk, N. Rubinina, and M. Woehlecke, *J. Opt. Soc. Am. B* **11**, 1681 (1994).

<sup>3</sup>T. Fujiwara, M. Takahashi, M. Ohama, A. J. Ikushima, Y. Furukawa, and J. Kitamura, *Electron. Lett.* **35**, 499 (1999).

<sup>4</sup>A. Grisard, E. Lallier, K. Polgár, and Á. Péter, *Electron. Lett.* **36**, 1043 (2000).

<sup>5</sup>V. Gopalan, T. E. Mitchell, Y. Furukawa, and K. Kitamura, *Appl. Phys. Lett.* **72**, 1981 (1998).

<sup>6</sup>Y. Furukawa, K. Kitamura, S. Takekawa, K. Niwa, and H. Hatano, *Opt. Lett.* **23**, 1892 (1998).

- <sup>7</sup>M. Fontana, K. Chah, M. Aillerie, and R. Mouras, *Opt. Mater. (Amsterdam, Neth.)* **16**, 111 (2000).
- <sup>8</sup>M. Sheik-Bahae, A. A. Said, T. H. Wei, D. J. Hagan, and E. W. Van Stryland, *IEEE J. Quantum Electron.* **26**, 760 (1990).
- <sup>9</sup>J. A. Hermann and R. G. McDuff, *J. Opt. Soc. Am. B* **10**, 2056 (1993).
- <sup>10</sup>L. Pálfalvi, G. Almási, J. Hebling, Á. Péter, and K. Polgár, *Appl. Phys. Lett.* **80**, 2245 (2002).
- <sup>11</sup>L. Pálfalvi, J. Hebling, G. Almási, Á. Péter, and K. Polgár, *J. Opt. A, Pure Appl. Opt.* **5**, S280 (2003).
- <sup>12</sup>K. Polgár, Á. Péter, I. Földvári, and Zs. Szaller, *J. Cryst. Growth* **218**, 327 (2000).
- <sup>13</sup>L. Kovács, G. Ruschhaupt, K. Polgár, G. Corradi, and M. Wöhlecke, *Appl. Phys. Lett.* **70**, 2801 (1997).
- <sup>14</sup>D. A. Bryan, R. Gerson, and H. E. Tomaschke, *Appl. Phys. Lett.* **44**, 847 (1984).
- <sup>15</sup>L. Kovács, K. Polgár, and R. Capelletti, *Cryst. Lattice Defects Amorphous Mater.* **15**, 115 (1987).
- <sup>16</sup>Q. W. Song, C. Zhang, and P. J. Talbot, *Appl. Opt.* **32**, 7266 (1993).
- <sup>17</sup>S. Bian, J. Frejlich, and H. H. Ringhofer, *Phys. Rev. Lett.* **78**, 4035 (1997).
- <sup>18</sup>S. Bian, *Opt. Commun.* **141**, 292 (1997).
- <sup>19</sup>P. P. Banerjee, R. M. Mirsa, and M. Maghraoui, *J. Opt. Soc. Am. B* **8**, 1072 (1991).
- <sup>20</sup>J. P. Gordon, R. C. C. Leite, R. S. Moore, S. P. Porto, and J. R. Whinnery, *J. Appl. Phys.* **36**, 3 (1965).
- <sup>21</sup>H. Li, F. Zhou, X. Zhang, and W. Ji, *Appl. Phys. B: Lasers Opt.* **64**, 659 (1997).
- <sup>22</sup>SNLO nonlinear optics code available from A. V. Smith, Sandia National Laboratories, Albuquerque, NM 87185-1423.